Effect of gravity on electrohydrodynamic (EHD) printing of silver nanoparticle and polycaprolactone based inks

Dewan Sal-Sabil Ahammed and Yang Cao

ELSEVIER

Available online at www.sciencedirect.com

Manufacturing Letters

Manufacturing Letters 44 (2025) 1000–1006

53rd SME North American Manufacturing Research Conference (NAMRC 53, 2025)

Effect of gravity on electrohydrodynamic (EHD) printing of silver nanoparticle and polycaprolactone based inks

Dewan Sal-Sabil Ahammed[a], Yang Cao[a*]

[a]Department of Mechanical and Industrial Engineering, Montana State University, Bozeman, MT 59717, USA

* Corresponding author. Tel.: +1-406-994-5942; E-mail address: yang.cao1@montana.edu

Abstract

Additive manufacturing is a promising technology to realize in-space manufacturing and long-duration manned space missions. Electrohydrodynamic (EHD) printing is an emerging additive manufacturing technology that offers high resolution and compatibility with a wide range of materials. A unique feature of EHD printing is that it does not rely on gravity for printing; instead, it uses a high electric field to induce fluid flows from micro capillary nozzles. Although gravity is not a determining factor in EHD printing, it can influence the printing process and performance. To make EHD printing a viable technology adaptable to different printing orientations and gravity magnitudes, it is essential to understand the effect of gravity on EHD printing. In this article, the effect of gravity on EHD printing of silver nanoparticle (AgNP) based ink and polycaprolactone dissolved in glacial acetic acid (PCL-GAA) ink were studied. Three printing orientations denoted as traditional, horizontal, and vertical setups were constructed in which the angle between the jetting direction and gravity direction were maintained at 0°, 90°, and 180°, respectively. The influence of gravity on critical voltage and printing resolution were studied through theoretical, experimental, and computational analyses. Results indicate that gravity has a noticeable impact on critical voltage and printing resolution. Compared with the traditional setup, the critical voltages are 5% and 10-25% higher, and the dimensions of printed patterns are 6-40% and 18-350% larger in the horizontal and vertical setups, respectively.

Keywords: *Electrohydrodynamic (EHD) printing, In-space manufacturing, Additive manufacturing, Gravity*

1. Introduction

Additive manufacturing (AM), also known as 3D printing, is a technology where parts are manufactured through depositing materials sequentially layer by layer. The high level of design flexibility, simple processing, and zero waste of AM make it well-suited for in-space manufacturing and long-duration manned space missions. Organizations such as the National Aeronautics and Space Administration (NASA) and European Space Agency (ESA) have attempted various implementations of AM for in-space manufacturing [1].

Electrohydrodynamic (EHD) printing is a high-resolution AM technology, in which a high electric field between the printing nozzle and the printing substrate causes the meniscus to deform into a conical shape known as Taylor cone [2], resulting in a printing resolution smaller than the nozzle's diameter [3–5]. Additionally, a key advantage of EHD printing is its ability to print inks with a broad range of viscosity from 1 to 1000 mPa·s and even over 20,000 mPa·s, whereas traditional inkjet printing can only print inks with viscosities of 1–10 mPa·s [6,7]. The high resolution and wide range of printable materials of EHD printing make it highly suitable for in-space manufacturing [8,9]. Another unique feature that makes EHD printing an excellent candidate for in-space manufacturing is that it does not rely primarily on gravity for printing; instead, it uses a high electric field to induce fluid flows from micro capillary nozzles.

A few pioneering studies have been conducted to explore the possibility of zero-gravity and anti-gravity EHD printing. Kirscht et al. [10] investigated the possibility of EHD printing in zero-gravity environment by conducting test on a parabolic flight. Under zero-gravity conditions, EHD printing maintained a stable Taylor cone jet, showing that electric forces alone could control material jetting even without gravity. However, in zero-gravity, higher electric fields were needed to produce the same print resolution as on Earth, due to the absence of gravitational influence on ink flow. Qu et al. [11] investigated the conditions needed for EHD printing in the anti-gravity environment. The study demonstrated that EHD printing could operate effectively in an anti-gravity setup, where high-voltage electrostatic forces enable stable jetting against the direction of gravity.

In the existing studies of EHD printing, the gravitational force has generally been neglected due to its limited influence when compared with other forces [12]. While evidence from electrospinning (the technology which EHD printing relies on) shows that gravity has a noticeable impact on various printing variables, such as the shape of the Taylor cone [13] and the diameter of printed filaments [14]. To make EHD printing a viable technology that can adapt to different printing orientations and gravity magnitudes (e.g., in-space, Moon, Mars, etc.), it is essential to understand the influence of gravity and develop corresponding control strategies to counterbalance the influence.

In this article, we investigated the influence of gravity on EHD printing of silver nanoparticle (AgNP) based ink and polycaprolactone dissolved in glacial acetic acid (PCL-GAA) ink. Three printing orientations, denoted as traditional, horizontal, and vertical setups, were constructed in which the angles between the jetting direction and the direction of gravity are 0, 90, and 180 degrees, respectively. First of all, the impact of gravity was investigated theoretically by analyzing the equilibrium of electrostatic force, surface tension, and gravity. Secondly, EHD printing experiments of AgNP and PCL inks were conducted in three different setups to quantitatively study the influence of gravity on critical voltage and printing resolution. Finally, finite element analysis (FEA) was conducted using COMSOL to further validate the results.

2. Theoretical Analysis

2.1 Theoretical model of EHD printing

In EHD printing, the printing ink is primarily driven by two categories of forces that act on the meniscus. The first type of forces are those that promote the jetting process towards the substrate, such as electrostatic force, and the second type of forces are those that resist the jetting process such as surface tension and viscous force [15]. Depending on the printing orientation, gravity can act as a promoting force (traditional setup), resisting force (vertical setup), or a perpendicular side force that has an effect only on the trajectory of the jet (horizontal setup). In this study, the "leaky-dielectric model" proposed by Taylor and Melcher is adopted for describing the EHD phenomenon [16]. A graphical description of the forces acting on the meniscus of EHD printing is illustrated in Fig. 1. Taylor's leaky dielectric model suggests that electric charges concentrate at the surface of the liquid at the nozzle tip without dispersing into the surrounding air. The applied electric field creates an electric force towards the substrate. The surface tension resisting the jet is counterbalanced by the normal

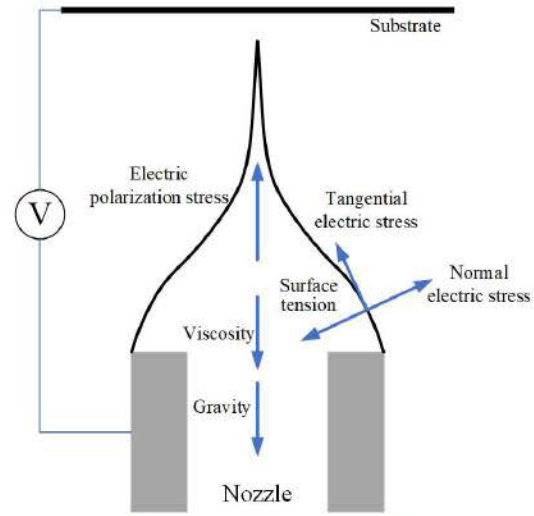

Fig. 1. Forces acting on the meniscus in EHD printing.

component of the generated electric stress. When the net promoting forces are greater than the net resisting forces, the printing ink is jetted and the ink material is deposited on the substrate.

2.2 Governing equations

In this section, we present the equations that govern the EHD phenomenon in EHD printing. The ink flow is described by the continuity and momentum equations, also referred to as the Navier-Stokes equations. For a Newtonian and incompressible fluid whose density ρ and viscosity μ are both constant, the continuity and momentum-conservation equations are written as follows [17–20]:

$$\nabla . \vec{u} = 0 \tag{1}$$

$$\rho\left(\frac{d\vec{u}}{dt} + \vec{u}.\nabla\vec{u}\right) = -\nabla P + \mu\nabla^2\vec{u} + F_g + F_e + F_{st} \tag{2}$$

where $\vec{u}$ represents fluid velocity. ρ, P, and μ represent the density, pressure, and viscosity, respectively. The terms F_g, F_e, and F_{st} denote the gravitational, electric, and surface tension forces, respectively. Among these forces, the electrostatic force F_e can be calculated using the Maxwell equation [21]:

$$F_e = \nabla . \vec{\sigma}^M = q_e\vec{E} - \frac{1}{2}\vec{E}.\vec{E}\nabla\varepsilon \tag{3}$$

where the terms $\vec{\sigma}^M, q_e, \vec{E}$, and ε correspond to the electrical stress tensor, charge intensity, electric field vector, and permittivity, respectively.

Additionally, the gravitational force F_g and surface tension F_{st} can be calculated using the following equations [22]:

$$F_g = \rho\,\vec{g} \tag{4}$$

$$F_{st} = \sigma\kappa\nabla.\hat{n} \tag{5}$$

where $\vec{g}$ denotes the gravitational acceleration, and $\sigma, \kappa, \hat{n}$ stand for the coefficient of surface tension, the surface curvature, and the unit normal vector of the surface.

To effectively track the dynamic liquid-air interface, the level set (LS) method is utilized. In this approach, a thin layer characterizes the interface, where the physical property transition from the liquid phase to the gas phase occurs. This method utilizes the non-conservative form to represent these variations, as expressed by the following equations [23].

$$\rho = \rho_a + (\rho_l - \rho_a)\emptyset \quad (6)$$

$$\varepsilon = \varepsilon_a + (\varepsilon_l - \varepsilon_a)\emptyset \quad (7)$$

$$\mu = \mu_a + (\mu_l - \mu_a)\emptyset \quad (8)$$

where the subscripts "*l*" and "*a*" are used to denote the liquid and gas phases, respectively. The term $\emptyset$ is introduced as the level-set function. Furthermore, ρ, ε, and μ refer to the density, electric permittivity, and viscosity, respectively.

2.3 Influence of gravity on EHD printing

Given the intricacy of the physics involved in EHD printing, most EHD printing models are based on scaling laws that establishes the relationship between printing parameters (e.g., voltage, printing speed) and printing variables (e.g., jet diameter, frequency) [12,24-25]. Scaling laws can be applied to find the relationship between gravity and printing resolution. Wang's theory [26] proposed an empirical formula that relates the printing width (*d*) to gravity (*g*):

$$d = Q^{\frac{1}{2}}\left[\frac{F}{\rho Q} + \left(\frac{2q_v V}{\rho Q r_c \ln\left(\frac{4H}{r_c}\right)}\right) + g\right]^{-\frac{1}{2}} \quad (9)$$

where the terms $\rho, Q, F_\mu, q_e, V, r_c, H, g$ represent the density, inner liquid volume, viscous force, charge intensity of free charges, applied electric potential, inner radius of the nozzle, printing distance, and gravity, respectively. From the above equation, it can be observed that the printing width or resolution has an inverse relation with viscous force, voltage, and gravity. In the case of the three setups in this study, the magnitude of gravity contributing to the jetting process can be positive (traditional setup), zero (horizontal setup), or negative (vertical setup). A closer examination of this equation reveals that a positive *g* in the traditional printing direction leads to a smaller printing width, compared with a negative *g* in the vertical setup and a zero *g* in the horizontal setup. Therefore, for EHD printing, it can be expected that a gravitational force along the jetting direction will increase the printing resolution, while a gravitational force acting against the jetting direction will decrease the printing resolution.

The EHD printing process is based on the interaction of promoting forces and resisting forces, and jetting happens when the promoting forces overcome the resisting forces. Before this stage, there is a point where equilibrium is reached between the promoting and resisting forces. This leads to the formation of the Taylor cone at the nozzle tip. The minimum voltage required to form the Taylor cone is known as the 'critical voltage'. Depending on the printing orientation, the component of the gravitational force in the jetting direction could be positive, negative, or zero (shown in Fig. 2). Hence, the electrostatic force required to counterbalance the surface tension would vary with the orientation of the setup. In the case of the traditional setup, the gravitational force is positive; hence, the required electrostatic force to counterbalance the surface tension would be lower. For the vertical setup, higher electrostatic force is required due to the resistive impact of gravity. For the horizontal setup, the direction of gravity is perpendicular to the jetting direction; hence, gravity has no direct influence on the magnitude of critical voltage.

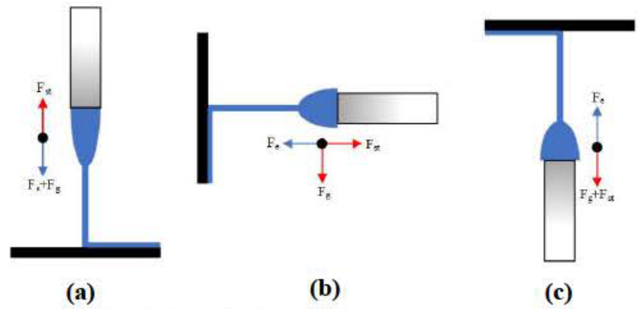

Fig. 2. Schematic of the three printing orientations in this study: a) traditional setup; b) horizontal setup; and c) vertical setup.

According to Eq. (3), for materials with uniform permittivity, the magnitude of the electric force is proportional to the applied electric field. In EHD printing, the relationship between the magnitude of the electric field and the applied voltage can be expressed by the equation [27]:

$$E = \frac{2V}{r_c \ln\left(\frac{4H}{r_c}\right)} \quad (10)$$

in which E, V, r_c, and H correspond to the electric field, applied voltage, inner radius of the nozzle, and standoff distance, respectively.

The critical voltage is an important process variable in EHD printing, which is the minimum voltage required to initiate the jetting process. Based on Eqs. (3) and (10), it can be deduced that gravity also has an influence on the magnitude of critical voltage. For the traditional setup, gravity acts along with the electrostatic force to overcome the resistive forces so that a lower critical voltage is needed. For the vertical setup, gravity acts against the printing direction, hence a higher critical voltage is required to overcome the enhanced overall resistive force. For the horizontal setup, the magnitude of critical voltage should be between those of traditional and vertical setups.

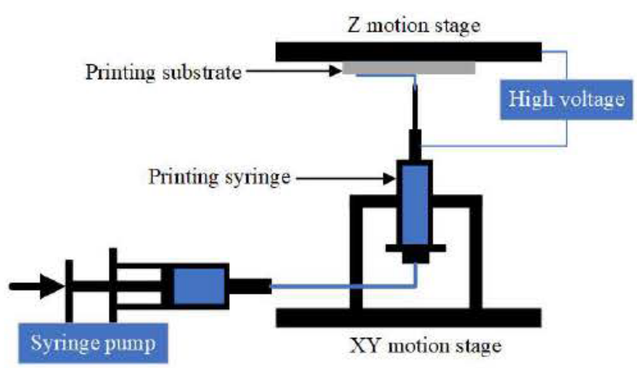

Fig. 3. Schematic of the experimental setup (vertical orientation).

3. Experimental Results

3.1 Materials

In this study, a commercial AgNP ink (Metalon JS-A102A, 40 wt.% Ag) was purchased from NovaCentrix, TX, USA. PCL (M_w = 50,000) was purchased from Scientific Polymer

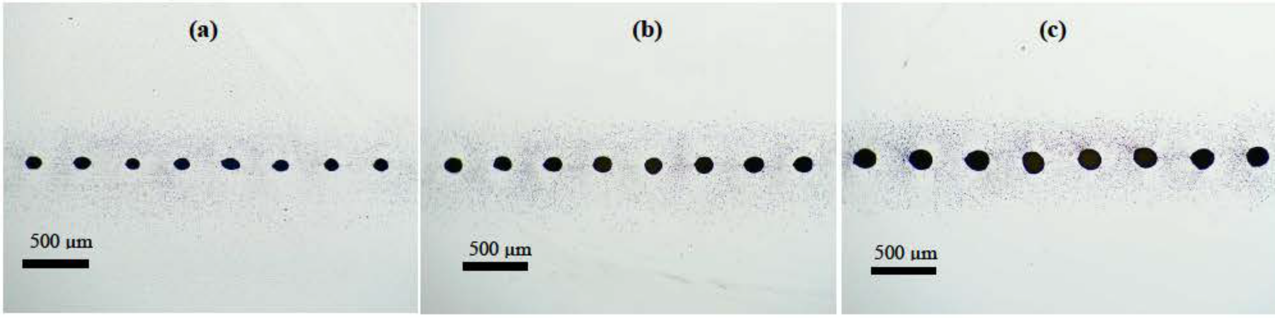

Fig. 4. EHD-printed AgNP droplets in a) traditional; b) horizontal; and c) vertical setups under the same experimental conditions.

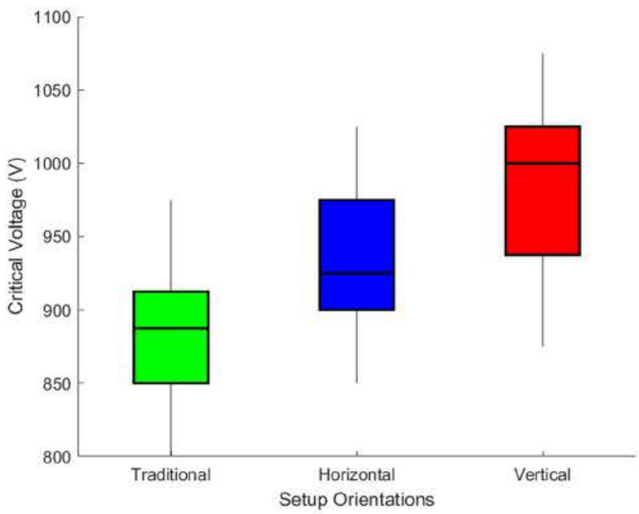

Fig. 5. Comparison of the critical voltage in EHD printing of AgNP ink in traditional, horizontal and vertical setups.

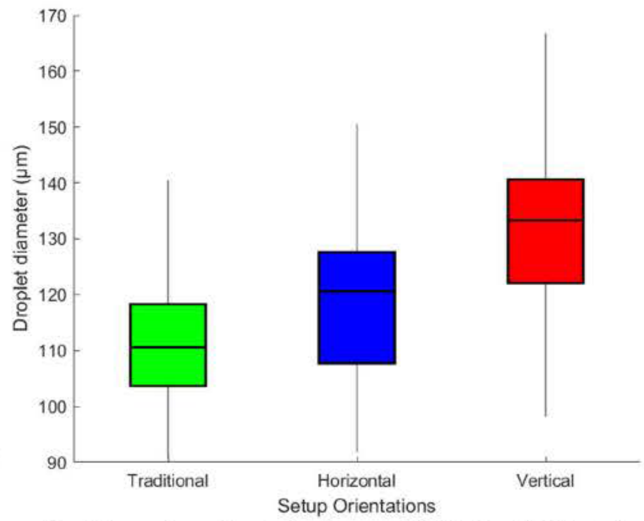

Fig. 6. Comparison of the droplet diameter of EHD-printed AgNP droplets in traditional, horizontal and vertical setups.

Products Inc. NY, USA. GAA (99%) was purchased from Lab Alley, TX, USA. All materials were used as received. 15 wt.% PCL-GAA solution was prepared by dissolving PCL in GAA and magnetically stirring the solution for 12 hours. The two inks were selected due to their distinct viscosities and applications. AgNP ink, printed in droplet mode, is commonly used to print electronics. PCL-GAA, printed in continuous jet mode, has been successfully used to print microscale 3D structures.

3.2 Experimental setup

The schematic of the experimental setup is shown in Fig. 3. The EHD printing system used in this study consists of an XYZ motion stage, a high-voltage power supply, a pneumatic dispersing system, and an optical microscopy system for process monitoring. The XYZ motion stage consists of three precision linear motors, which can travel up to 250 mm, 250 mm, and 80 mm in X, Y, and Z directions with a motion resolution less than 1 µm. A waveform generator (Rigol DG822) was used to provide the necessary electrical signal, which is amplified by a high-voltage power supply (Stanford Research Systems, PS-350). A programmable syringe pump (SyringeONE, NE-1010) was used to pump the printing syringe and supply a constant flow rate while moving the ink through the connecting tubes to the printing nozzle. Nozzles with inner diameters of 0.16 mm and 0.52 mm were used for dispensing the AgNP ink and the PCL-GAA ink, respectively. For droplet deposition of AgNP, a voltage of 1.6 kV, a frequency of 0.3 Hz, and a duty cycle of 40% were applied. The programmable syringe pump was utilized to maintain a consistent flow rate of 3 µL/hr. A printing speed and printing distance of 5 mm/min and 0.25 mm respectively were kept constant throughout the experiment. For the PCL-GAA ink, the flow rate applied was set to be 0.2 mL/hr. The standoff distance was kept constant at 1.15 mm and the printing speed was maintained at 125 mm/min. An electric potential of 2.4 kV magnitude was applied for the continuous jet printing of the PCL-GAA ink.

3.3 Results and discussion

Fig. 4 shows the EHD-printed AgNP droplets in the three experimental setups. Fig. 5 shows the range of critical voltages required for stable EHD printing of AgNP ink in the three different setups. In the traditional setup, gravity acts along with the electrostatic force to overcome surface tension, thus requiring the lowest voltage range from 800 to 975 V. The horizontal orientation requires a slightly higher critical voltage, ranging from 850 to 1025 V. The vertical setup requires the highest critical voltage, ranging from 875 to 1075 V. The average critical voltage for the traditional, horizontal and vertical setups are 885 V, 930 V, and 981 V, respectively. Fig. 6 compares the diameter of printed AgNP droplets in the three different setups under the same experimental conditions as described in Section 3.2. The results reveal distinct differences in droplet size based on setup orientations. In the traditional setup, the average droplet diameter was the smallest at 111.47 µm. The horizontal setup yielded a slightly larger average

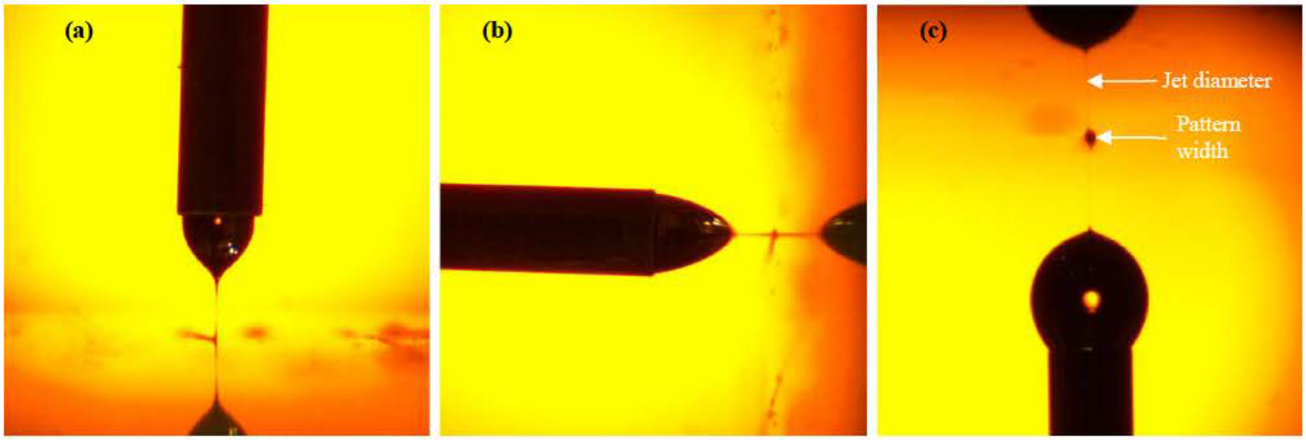

Fig. 7. Taylor cone of EHD printing of the PCL-GAA ink in a) traditional; b) horizontal; and c) vertical setups under the same experimental conditions.

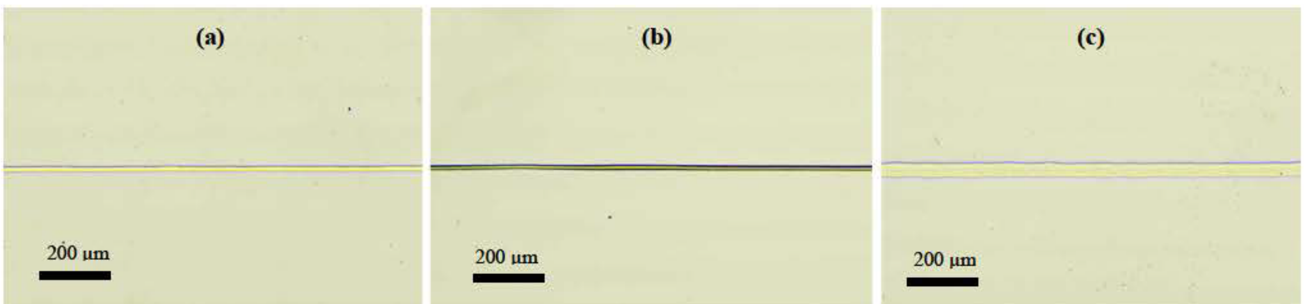

Fig. 8. EHD-printed line samples using the PCL-GAA ink in a) traditional; b) horizontal; and c) vertical setups under the same experimental conditions.

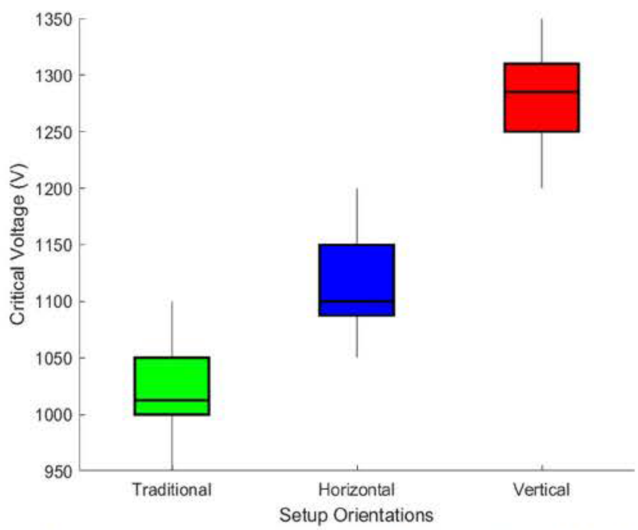

Fig. 9. Comparison of the critical voltage in EHD printing of PCL-GAA ink in traditional, horizontal and vertical setups.

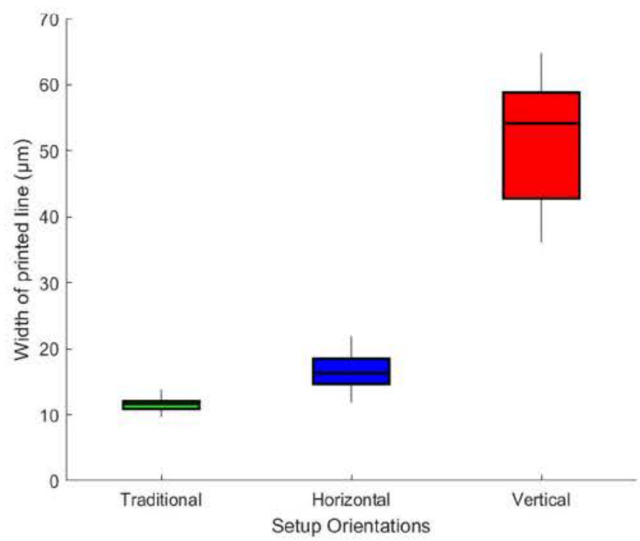

Fig. 10. Comparison of the line width in EHD printing of PCL-GAA ink in traditional, horizontal and vertical setups.

droplet diameter of 118.55 µm. The vertical setup deposited the largest droplets, with an average diameter of 131.94 µm.

Micrographs of the Taylor cone for the three setups in the EHD printing of PCL-GAA ink are presented in Fig. 7. In the traditional setup, the Taylor cone is more elongated due to the influence of gravity acting along the printing direction. In the horizontal setup, the Taylor cone is slightly asymmetric, which is caused by gravity acting perpendicular to the flow. In the vertical setup, where the ink moves upward against gravity, the Taylor cone is more compressed. It is also worth noting that the jet diameter and pattern width are different, with the latter usually being several times larger than the former. Based on experimental results, it was found that the pattern width is approximately 2.96, 3.50, and 6.50 times the jet diameter in the traditional, horizontal, and vertical setups, respectively.

Fig. 8 shows the printed lines using the PCL-GAA ink in the traditional, horizontal, and vertical setups. The comparison of the critical voltage of the three setups is depicted in Fig. 9, which shows a similar trend to the printing of the AgNP ink. The traditional setup has the lowest critical voltage, ranging from 950 to 1100 V, with an average of 1022.5 V. In the horizontal setup, the critical voltage ranges from 1050 to 1200 V, with an average of 1107.5 V. The vertical setup requires the highest voltage, ranging from 1200 to 1350 V with an average of 1282.5 V. Fig. 10 compares the line width of the printed samples using the PCL-GAA ink in the three different setups under the same experimental conditions as described in Section 3.2, which shows a similar trend as the diameter of EHD-printed AgNP droplets. In the traditional setup, the average line width is 11.57 µm. In the horizontal setup, the average line width increases to 16.66 µm. The vertical setup deposits the largest line width with an average value of 52.01 µm.

4. Simulation Results

To further investigate the gravitational effect on the EHD printing process, an FEA model was developed using COMSOL Multiphysics 6.2. This model, based on the leaky-dielectric model by Taylor and Melcher [16], was created by combining a laminar flow model, an electrostatic model, and a level set module to solve the coupled Navier-Stokes equation and electrostatic equations, as validated by prior studies [3,11].

Since the cylindrical nozzle is symmetric with respect to the central axis, an axisymmetric model was formulated to decrease the computation time. The simulation incorporated a stainless-steel nozzle as the positive electrode and a glass substrate as the grounded terminal. The material properties of stainless steel and glass were sourced from COMSOL's materials library. The interior of the printing nozzle was defined as the printing ink, and the remaining space of the domain was set as air. The AgNP ink's physical properties were obtained from the supplier's datasheet, including density 1630 kg/m³, viscosity 0.01 Pa·s, and surface tension 0.0197 N/m. The ink is composed of 40 w% AgNP nanoparticles, 30 w% water, and 30 w% diethylene glycol. The dielectric constant was estimated to be 55.7 using Jouyban's theory [28]. The simulation results of AgNP ink are presented in Fig. 11. The three models have the exact same configurations except for the direction of gravity. The simulated jet diameters were 27.45 µm for the traditional setup, 29.1 µm for the horizontal setup, and 35.5 µm for the vertical setup. Note that the simulated results are the jet diameter, while the experimental results shown in Fig. 6 are the diameter of the deposited AgNP droplets, which is usually several times larger than the jet diameter. A comparison of their relative values reveals that droplets in the horizontal and vertical setups are 106.01% and 129.32% larger than those in the traditional setup. This trend is consistent with the experimental results, which show that the average droplet diameters in horizontal and vertical setups are 106.35% and 118.29% greater than those in the traditional setup.

The PCL-GAA ink is composed of 15 w% PCL in GAA. Based on the densities of PCL 1145 kg/m³ and GAA 1049 kg/m³ from suppliers' datasheet, the density of PCL-GAA ink is calculated to be 1062 kg/m³. Other properties such as viscosity, surface tension, and dielectric constant are found to be 0.891 Pa·s, 0.03 N/m, and 6.2, respectively, from previous literature [29]. The simulation results for the PCL-GAA ink are shown in Fig. 12. The simulated jet diameters for the traditional, horizontal, and vertical setups were 5.1, 5.8, and 7.1 µm, respectively. By multiplying the constant factor between the jet diameter and pattern width for each setup as explained in Section 3.3, the simulated line widths can be estimated to be 15.10, 20.30, and 46.15 µm for the traditional, horizontal, and vertical setups, which closely align with the experimental results.

5. Conclusions

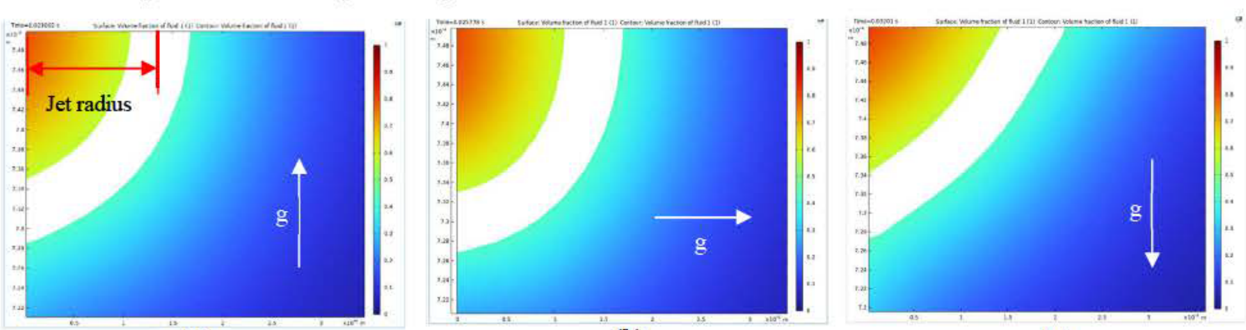

(a) (b) (c)

Fig. 11. Simulated axisymmetric AgNP jet radius in a) traditional; b) horizontal; and c) vertical setups.

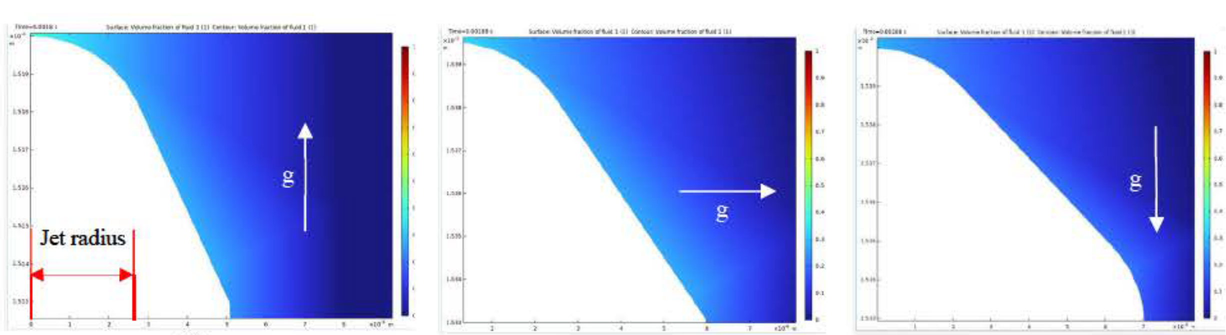

(a) (b) (c)

Fig. 12. Simulated axisymmetric PCL-GAA jet radius in a) traditional; b) horizontal; and c) vertical setups.

In this study, we investigated the influence of gravity on EHD printing, specifically the critical voltage and printing resolution. First of all, we theoretically analyzed the influence of gravity on the EHD printing process. To quantify the influence of gravity, we conducted a series of experiments using an AgNP ink and a PCL-GAA polymeric ink. Due to their different rheological and dielectric properties, the AgNP ink was printed as droplets, while the PCL-GAA ink was printed as filaments. The investigation was based on three different setups: traditional, horizontal, and vertical, where the angle between the jetting direction and gravity was maintained at 0°, 90°, and 180°, respectively. The experimental results revealed that gravity has a noticeable impact on both the critical voltage and printing resolution. Compared with the traditional setup, the critical voltage required for the horizontal setup for both inks are approximately 5% higher, while the critical voltage for the vertical setup is 10% higher for the AgNP ink and about 25% higher for the PCL-GAA ink. For the printed patterns, the dimensions of the AgNP droplets using the horizontal and vertical setup are approximately 6.35% and 18.36% larger than the droplets in the traditional setup, respectively. In the case of the PCL-GAA printed lines, the width of the printed lines for the horizontal and vertical setups were 40% and 350% wider than the lines printed in the traditional setup. These trends were further validated through FEA simulations. These findings provide valuable insights for implementing EHD printing in future in-space manufacturing applications where the orientation and magnitude of gravity might vary significantly.

References

[1] Sacco E, Moon SK. Additive manufacturing for space: status and promises. Int J Adv Manuf Technol 2019;105(10):4123–46.

[2] Taylor GI. Electrically driven jets. Proc R Soc Lond A Math Phys Sci 1969;313(1515):453–75.

[3] Jiang L, Yu L, Premaratne P, Zhang Z, Qin H. CFD-based numerical modeling to predict the dimensions of printed droplets in electrohydrodynamic inkjet printing. J Manuf Process 2021;66:125–32.

[4] Park JU, Hardy M, Kang SJ, Barton K, Adair K, Mukhopadhyay DK, Lee CY, Strano MS, Alleyne AG, Georgiadis JG, Ferreira PM. High-resolution electrohydrodynamic jet printing. Nat Mater 2007;6(10):782–9.

[5] Huang Y, Cao Y, Qin H. Electric field assisted direct writing and 3D printing of low - melting alloy. Adv Eng Mater 2022;24(9).

[6] Kwon J, Hong S, Suh YD, Yeo J, So HM, Chang WS, Ko SH. Direct micro metal patterning on plastic substrates by electrohydrodynamic jet printing for flexible electronic applications. ECS J Solid State Sci Technol 2015;4(4) –P3056.

[7] Krainer S, Smit C, Hirn U. The effect of viscosity and surface tension on inkjet printed picoliter dots. RSC Adv 2019;9(54):31708–19.

[8] Reiser A, Lindén M, Rohner P, Marchand A, Galinski H, Sologubenko AS, Wheeler JM, Zenobi R, Poulikakos D, Spolenak R. Multi-metal electrohydrodynamic redox 3D printing at the submicron scale. Nat Commun 2019;10(1):1853.

[9] Jiang L, Li W, Wolf R, Marander M, Kirscht T, Liu F, Jones JM, Hill C, Jiang S, Qin H. High-sensitivity fully printed flexible BaTiO3-based capacitive humidity sensor for in-space manufacturing by electrohydrodynamic inkjet printing. IEEE Sens J 2024;24(15):24659–67.

[10] Kirscht T, Jiang L, Liu F, Jiang X, Marander M, Ortega R, Qin H, Jiang S. Silver Nano-inks synthesized with biobased polymers for high-resolution electrohydrodynamic printing toward in-space manufacturing. ACS Appl Mater Interfaces 2024;16(33):44225–35.

[11] Qu M, Meng Z, Gao T, He J, Li D. Exploration of electrohydrodynamic printing potentially for in-space fabrication of microscale functional structures: A preliminary study by an anti-gravity configuration. Addit Manuf 2023;61:103349.

[12] Choi HK, Park JU, Park OO, Ferreira PM, Georgiadis JG, Rogers JA. Scaling laws for jet pulsations associated with high-resolution electro-hydrodynamic printing. Appl Phys Lett 2008;92(12).

[13] Suresh S, Becker A, Glasmacher B. Impact of apparatus orientation and gravity in electrospinning—A review of empirical evidence. Polymers 2020;12(11):2448.

[14] Yang C, Jia Z, Xu Z, Wang K, Guan Z, Wang L. Comparisons of fibers properties between vertical and horizontal type electrospinning systems. In: 2009 IEEE Conference on Electrical Insulation and Dielectric Phenomena. IEEE; 2009. p. 204–7.

[15] Farjam N, Spiegel IA, Barton K. High-fidelity modeling and validation of electrohydrodynamic jet printing. Materialia 2022;26:101578.

[16] Saville DA. The Taylor-Melcher leaky dielectric model. Annu Rev Fluid Mech 1997;29(1):27–64.

[17] Gurtin EM. An introduction to continuum mechanics. San Diego: Academic Press Inc.; 1981.

[18] Landau LD. Fluid Mechanics. 2nd ed. Oxford: Butterworth-Heinemann; 1999.

[19] Batchelor GK. An introduction to fluid dynamics. Cambridge: Cambridge University Press; 1990.

[20] Massey BS. Mechanics of Fluids. 6th ed. London: Chapman & Hall; 1989.

[21] Lastow O, Balachandran W. Numerical simulation of electrohydrodynamic (EHD) atomization. J Electrostat 2006;64(12):850–9.

[22] Paul A, Shekhar Roy S. Numerical simulation to predict printed width in EHD inkjet 3D printing process. Mater Today Proc 2022;62:373–9.

[23] Hochleitner G, Jüngst T, Brown TD, Hahn K, Moseke C, Jakob F, Dalton PD, Groll J. Additive manufacturing of scaffolds with sub-micron filaments via melt electrospinning writing. Biofabrication 2015;7(3):035002.

[24] Chen CH, Saville DA, Aksay IA. Scaling laws for pulsed electrohydrodynamic drop formation. Appl Phys Lett 2006;89(12).

[25] An S, Lee MW, Kim NY, Lee C, Al-Deyab SS, James SC, Yoon SS. Effect of viscosity, electrical conductivity, and surface tension on direct-current-pulsed drop-on-demand electrohydrodynamic printing frequency. Appl Phys Lett 2014;105(21).

[26] Wang D, Lu L, Zhao Z, Zhao K, Zhao X, Pu C, Li Y, Xu P, Chen X, Guo Y, Suo L. Large area polymer semiconductor sub-microwire arrays by coaxial focused electrohydrodynamic jet printing for high-performance OFETs. Nat Commun 2022;13(1):6214.

[27] Kebarle P, Verkerk UH. Electrospray: From ions in solution to ions in the gas phase, what we know now. Mass Spectrom Rev 2009;28(6):898–917.

[28] Jouyban A, Soltanpour S, Chan HK. A simple relationship between dielectric constant of mixed solvents with solvent composition and temperature. Int J Pharm 2004;269(2):353–60.

[29] Li W, Shi L, Zhang X, Liu K, Ullah I, Cheng P. Electrospinning of polycaprolactone nanofibers using H_2O as benign additive in polycaprolactone/glacial acetic acid solution. J Appl Polym Sci 2018;135(3).